

# Synthesis of Rare Earth Polyborates Using Molten Boric Acid as a Flux

Linyan Li,<sup>†</sup> Peichao Lu,<sup>†</sup> Yaoyang Wang,<sup>†</sup> Xianglin Jin,<sup>‡</sup> Guobao Li,<sup>†</sup> Yingxia Wang,<sup>†</sup> Liping You,<sup>§</sup> and Jianhua Lin<sup>\*,†</sup>

State Key Laboratory of Rare Earth Materials Chemistry and Applications,  
College of Chemistry and Molecular Engineering, State Key Laboratory of Molecular Dynamic  
and Stable Structures, College of Chemistry and Molecular Engineering, and Electron  
Microscopy Laboratory, Department of Physics, Peking University,  
Beijing 100871, People's Republic of China

Received April 15, 2002. Revised Manuscript Received October 1, 2002

Hydrated rare earth hexaborates  $H_3LnB_6O_{12}$  ( $Ln = Sm-Lu$ ) have been synthesized by using molten boric acid as the reaction medium.  $H_3LnB_6O_{12}$  decomposes at certain temperatures to form anhydrous pentaborates  $LnB_5O_9$  ( $Ln = Sm-Er$ ) or orthoborates  $LnBO_3$  ( $Ln = Tm-Lu$ ). The crystal structures of the hexaborates and pentaborates have been determined by single-crystal and powder diffraction techniques. The hydrated hexaborates  $H_3LnB_6O_{12}$  crystallize in a trigonal structure in the space group  $R\bar{3}c$ , which contain a six-membered ring  $B_6O_{15}$  as a fundamental fragment. Anhydrous pentaborates  $LnB_5O_9$  crystallize in a tetragonal structure that is built up with  $B_4O_9$  and  $BO_3$ .  $LnB_5O_9$  decomposes at higher temperature to metaborates ( $Ln = Sm-Tb$ ) and orthoborates ( $Ln = Dy-Er$ ). A phase diagram is presented that shows the stable range of both  $H_3LnB_6O_{12}$  and  $LnB_5O_9$ . The luminescent property of the europium-doped  $GdB_5O_9$  was studied.

## Introduction

Borates have long been the subject of interest over many decades, motivated by their extraordinary optical properties. Many borates are transparent in a wide spectrum with high nonlinear optical coefficients due to the strong covalent B–O bond and diverse structures. The syntheses of borates can be readily achieved either by high-temperature reaction or in aqueous solution. According to the Lux-Flood acid–base concept, anhydrous polyborates are less stable for the small-size and high-valence cations;<sup>1</sup> therefore, high-temperature syntheses often failed for some polyborate systems. Rare earth borates are one of the typical examples, wherein only three compounds were identified by high-temperature reaction in the  $Ln_2O_3-B_2O_3$  ( $Ln =$  rare earth) system.<sup>2</sup> The oxyborates<sup>3,4</sup> and orthoborates<sup>5,6</sup> are stable at high temperature for all rare earths. The stability of the metaborates<sup>7</sup> declines with the decrease of the cation size to the point that the metaborates of heavy rare

earths (Dy–Lu) are not present. Considering the diversity of the polyborate groups, more boron-rich rare earth polyborates may exist, but they may not be stable at high temperature. One possible approach for obtaining rare earth polyborates is to carry out the reaction at low temperature in a controlled manner.

Boric acid melts at about 171 °C and it does preserve most desirable requirements as a reaction medium for polyborates. Recently, we found that boric acid is indeed a suitable reaction medium, in which several novel rare earth polyborates were obtained.<sup>8</sup> Here in this report, we describe the syntheses and structure characterization of the hydrated rare earth hexaborates  $H_3LnB_6O_{12}$  ( $Ln = Sm-Lu$ ). Careful dehydration of  $H_3LnB_6O_{12}$  at mild conditions resulted in boron-rich anhydrous pentaborates  $LnB_5O_9$  ( $Ln = Sm-Er$ ).

## Experimental Section

**General Procedure.**  $H_3LnB_6O_{12}$  ( $Ln = Sm-Lu$ ) were synthesized by using  $H_3BO_3$  (analytical grade) and  $Ln_2O_3$  (99.99%) as the starting materials. DTA and TGA measurements were carried out on a Dupont 1090 instrument. IR spectra were recorded on a Nickel Magna-750 FT-IR spectrometer. Luminescent spectra under VUV excitation were recorded at Beijing Synchrotron Radiation Laboratory, using sodium salicylate as a standard. Powder X-ray diffraction patterns were recorded on a Rigaku D/max-2000 diffractometer with graphite monochromatized  $Cu K\alpha$  radiation at 50 kV, 120 mA.

**Synthesis of Hydrated Hexaborates  $H_3LnB_6O_{12}$  ( $Ln = Sm-Lu$ ).**  $H_3BO_3$  and  $Ln_2O_3$  in a mole ratio of 60:1 were mixed

\* To whom correspondence should be addressed. E-mail: jhlin@chem.pku.edu.cn. Tel.: (8610)62751715. Fax: (8610)62751708.

<sup>†</sup> State Key Laboratory of Rare Earth Materials Chemistry and Applications, College of Chemistry and Molecular Engineering.

<sup>‡</sup> State Key Laboratory of Molecular Dynamic and Stable Structures, College of Chemistry and Molecular Engineering.

<sup>§</sup> Electron Microscopy Laboratory, Department of Physics.

(1) Leonyuk, N. I. *J. Cryst. Growth* **1997**, *174*, 301.

(2) Levin, E. M.; Robbins, C. R.; Warring, J. L. *J. Am. Ceram. Soc.* **1961**, *44*, 87.

(3) Lin, J. H.; Su, M. Z.; Wurst, K.; Schweda, E. *J. Solid State Chem.* **1996**, *126*, 287.

(4) Lin, J. H.; Zhou, S.; Yang, L. Q.; Yao, G. Q.; Su, M. Z.; You, L. P. *J. Solid State Chem.* **1997**, *134*, 158.

(5) Ren, M.; Lin, J. H.; Dong, Y.; Yang, L. Q.; Su, M. Z.; You, L. P. *Chem. Mater.* **1999**, *11*, 1576.

(6) Yang, Z.; Ren, M.; Lin, J. H.; Su, M. Z.; Tao, Y.; Wang, W. *Chem. J. Chin. Univ. (Chinese)* **2000**, *21* (9), 1339.

(7) Abdullaev, G. K.; Mamedov, Kh. S.; Dzhafarov, G. G. *Sov. Phys. Crystallogr.* **1975**, *20*, 161.

(8) Lu, P. C.; Wang, Y. X.; Lin, J. H.; You, L. P. *Chem. Commun.* **2001**, 1178.

**Table 1. Crystal Data and the Structure Refinement of  $H_3GdB_6O_{12}$  and  $GdB_5O_9$** 

formula	$H_3GdB_6O_{12}$	$GdB_5O_9$
formula mass	417.13	355.30
crystal system	trigonal	tetragonal
space group	$R\bar{3}c$	$I\bar{4}_1/acd$
$a$ (Å)	8.405(1)	8.23813(6)
$c$ (Å)	20.771(4)	33.6377(4)
$V$ (Å $^3$ )	1270.8(3)	2282.88(4)
$Z$	6	16
density (calc.) (g/cm $^3$ )	3.27	4.135
diffraction technique	single-crystal diffraction	powder X-ray diffraction
reflections	3228 of which 1014 are unique	5399 profile data, 293 reflections
structure determination and refinement	direct method, SHELXL 97	direct method, EXTRa, Sirpow, and GSAS
$R$ indices ( $I > 2\sigma$ )	$R_1 = 0.0260$ , $wR_2 = 0.0617$	$R_p = 0.0548$ , $R_{wp} = 0.0782$

**Table 2. Atomic Coordinates and Isotropic Thermal Displacement Parameters in  $H_3GdB_6O_{12}$** 

atom	site	$x$	$y$	$z$	$U$ (eq)
Gd1	3a	1/3	2/3	0.0797(2)	0.009(1)
O1	18b	0.5279(6)	0.5290(6)	-0.0531(2)	0.012(1)
O2	18b	0.8644(5)	0.7727(7)	-0.1693(2)	0.013(1)
O3	18b	0.4923(5)	0.3999(4)	-0.1784(1)	0.013(1)
O4	18b	0.2416(3)	0.3227(4)	-0.1043(1)	0.011(1)
B1	18b	0.6284(6)	0.6664(7)	-0.0027(3)	0.011(1)
B2	18b	0.7571(6)	0.7646(6)	-0.2203(3)	0.012(1)

and charged into Teflon autoclaves. The reactions were carried out at 240 °C for about 5 days. The excess boric acid was removed by washing the products with distilled water, and the products were then dried at 80 °C for 10 h. Chemical analysis (ICP method) shows that the B:Ln ratio is approximately 6:1, and IR spectra indicate the presence of both  $BO_3$  and  $BO_4$  groups<sup>9,10</sup> in the products. Crystals used for single-crystal structure determination were obtained in a similar fashion. A small amount of water ( $H_2O:H_3BO_3:Ln_2O_3 = 60:60:1$ ) was found to be helpful for obtaining single crystals.

**Synthesis of Anhydrous Pentaborates  $LnB_5O_9$  (Ln = Sm–Er).** Anhydrous pentaborates  $LnB_5O_9$  (Ln = Sm–Er) were obtained by heating  $H_3LnB_6O_{12}$  at 650–700 °C for 5 days. Decomposition of the hydrated hexaborates of the heavy rare earth (Ln = Tm, Yb, and Lu) resulted in the orthoborates, instead of the pentaborates. IR spectroscopy confirms that the pentaborates contain both  $BO_3$  and  $BO_4$ .<sup>9,10</sup>

**X-ray Crystallographic Study.** A crystal of  $H_3GdB_6O_{12}$  of about  $0.15 \times 0.15 \times 0.15$  mm $^3$  was used for single-crystal diffraction data collection on a Rigaku R-AXIS RAPID image plate diffractometer with graphite monochromated Mo  $K\alpha$  radiation ( $\lambda = 0.71073$  Å). The data set was collected up to  $2\theta = 54.7^\circ$  and absorption correction was applied based on symmetry-equivalent reflections using the ABSOR program<sup>11</sup> (1014 unique reflections,  $R_{int} = 0.0436$ ).  $H_3GdB_6O_{12}$  crystallizes in space group  $R\bar{3}c$ . The unit cell parameters, derived by indexing performed from two oscillation images, are  $a = 8.405(1)$  Å and  $c = 20.771(4)$  Å. The structure was solved by direct method (SHELXS97) and refined by full-matrix least-squares refinement.<sup>12</sup> Crystallographic data and refined parameters are listed in Table 1. The atomic coordinates and selected bond lengths and angles are listed in Tables 2 and 3, respectively. All other hexaborates  $H_3LnB_6O_{12}$  (Ln = Sm, Eu, Tb, Dy, Ho, Er, Tm, Yb, and Lu) are isostructural to  $H_3GdB_6O_{12}$  as confirmed by powder X-ray diffraction patterns.

Pentaborates  $LnB_5O_9$  were obtained by decomposition of  $H_3LnB_6O_{12}$ , so it is impossible to obtain crystals suitable for single-crystal structure determination. The crystal structure of  $GdB_5O_9$  was established by an ab initio method using powder X-ray diffraction data. The powder X-ray diffraction

**Table 3. Selected Bond Distances (Å) and Angles (deg) for  $H_3GdB_6O_{12}$** 

	bond distance (Å)	bond angles (deg)
Gd1–O2	3	2.387(5)
Gd1–O3	3	2.392(4)
Gd1–O4	3	2.470(3)
B1–O1	1.472(7)	O3–B1–O2
B1–O2	1.509(5)	O1–B1–O2
B1–O3	1.449(6)	O4–B1–O2
B1–O4	1.479(5)	O1–B2–O4
B2–O1	1.363(6)	O1–B2–O2
B2–O2	1.370(7)	O4–B2–O2
B2–O4	1.369(6)	

pattern of  $GdB_5O_9$  was indexed with a tetragonal cell  $a = 8.23813(6)$  Å and  $c = 33.6377(4)$  Å with PowderX.<sup>13</sup> Careful inspection of the reflections revealed that the only possible space group is  $I\bar{4}_1/acd$ . Optimal estimates of the individual reflection intensities were extracted by a profile-fitting method using EXTRa.<sup>14</sup> A total of 239 reflections were extracted in the range of  $2\theta < 90^\circ$ , of which 91 are independent. The initial structure model was established by a direct method (Sirpow92<sup>15</sup>), and at this stage, nine crystallographic positions, that is, one Gd atom, five O atoms, and three B atoms, were located directly from the E-map. Different Fourier analysis was carried out and used to locate the rest of the oxygen positions (GSAS<sup>16</sup>). The final refinement, with isotropic thermal displacement parameters, yielded  $R_p = 0.0548$  and  $R_{wp} = 0.0782$ . Figure 1 shows the profile fit of the diffraction pattern, the crystallographic data are listed in Table 1, and the atomic coordinates and selected bond lengths and angles are listed in Tables 4 and 5. All other pentaborates  $LnB_5O_{12}$  (Ln = Sm, Eu, Tb, Dy, Ho, and Er) are isostructural to  $GdB_5O_9$  as confirmed by powder X-ray diffraction patterns.

## Results and Discussions

Reaction of rare earth oxides and boric acid in molten boric acid is a simple acid–base reaction but is effective for producing rare earth polyborates. When heated in an open vessel, boric acid dehydrates stepwise and polymerizes to metaboric acid and then to boron oxide.<sup>17–24</sup> The typical polymerization process from boric

(9) Laperches, J. P.; Tarte, P. *Spectrochim. Acta* **1966**, *22*, 1201.

(10) Denning, J. H.; Ross, S. D. *Spectrochim. Acta* **1972**, *28A*, 1775.

(11) Higashi, T. *ABSCOR, Empirical Absorption based on Fourier Series Approximation*; Rigaku Corporation: Tokyo, 1995.

(12) Sheldrick, G. M. *SHELXS 97, Program for the solution of crystal structures*; University of Göttingen: Göttingen, Germany, 1997.

(13) Dong, C. *J. Appl. Crystallogr.* **1999**, *32*, 838.

(14) Altomare, A.; Burla, M. C.; Cascarano, G.; Giacovazzo, C.; Guagliardi, A.; Molterni, A. G. G.; Polidori, G. *J. Appl. Crystallogr.* **1995**, *28*, 842.

(15) Altomare, A.; Cascarano, G.; Giacovazzo, C.; Guagliardi, A. *SIRPOW user's manual*; Inst. Di Ric. Per lo Sviluppo di Metodologie Cristallografiche, CNR.

(16) Larson, A. C.; von Dreele, R. B. Report LAUR 86-748; Los Alamos National Laboratory: Los Alamos, NM, 1985.

(17) Wells, A. F. *Structural Inorganic Chemistry*, 5th ed.; Oxford University Press: Oxford, 1984; p 1045.

(18) Craven, B. M.; Sabine, T. M. *Acta Crystallogr.* **1966**, *20*, 214.

(19) Peters, C. R.; Milberg, M. E. *Acta Crystallogr.* **1964**, *17*, 229.

(20) Zachariasen, W. H. *Acta Crystallogr.* **1963**, *16*, 385.

(21) Zachariasen, W. H. *Acta Crystallogr.* **1963**, *16*, 380.

(22) Gurr, G. E.; Montgomery, P. W.; Knutson, C. D.; Gorres, B. T. *Acta Crystallogr.* **1970**, *B26*, 906.

(10) Denning, J. H.; Ross, S. D. *Spectrochim. Acta* **1972**, *28A*, 1775.

(11) Higashi, T. *ABSCOR, Empirical Absorption based on Fourier Series Approximation*; Rigaku Corporation: Tokyo, 1995.

(12) Sheldrick, G. M. *SHELXS 97, Program for the solution of crystal structures*; University of Göttingen: Göttingen, Germany, 1997.

(13) Dong, C. *J. Appl. Crystallogr.* **1999**, *32*, 838.

(14) Altomare, A.; Burla, M. C.; Cascarano, G.; Giacovazzo, C.; Guagliardi, A.; Molterni, A. G. G.; Polidori, G. *J. Appl. Crystallogr.* **1995**, *28*, 842.

(15) Altomare, A.; Cascarano, G.; Giacovazzo, C.; Guagliardi, A. *SIRPOW user's manual*; Inst. Di Ric. Per lo Sviluppo di Metodologie Cristallografiche, CNR.

(16) Larson, A. C.; von Dreele, R. B. Report LAUR 86-748; Los Alamos National Laboratory: Los Alamos, NM, 1985.

(17) Wells, A. F. *Structural Inorganic Chemistry*, 5th ed.; Oxford University Press: Oxford, 1984; p 1045.

(18) Craven, B. M.; Sabine, T. M. *Acta Crystallogr.* **1966**, *20*, 214.

(19) Peters, C. R.; Milberg, M. E. *Acta Crystallogr.* **1964**, *17*, 229.

(20) Zachariasen, W. H. *Acta Crystallogr.* **1963**, *16*, 385.

(21) Zachariasen, W. H. *Acta Crystallogr.* **1963**, *16*, 380.

(22) Gurr, G. E.; Montgomery, P. W.; Knutson, C. D.; Gorres, B. T. *Acta Crystallogr.* **1970**, *B26*, 906.

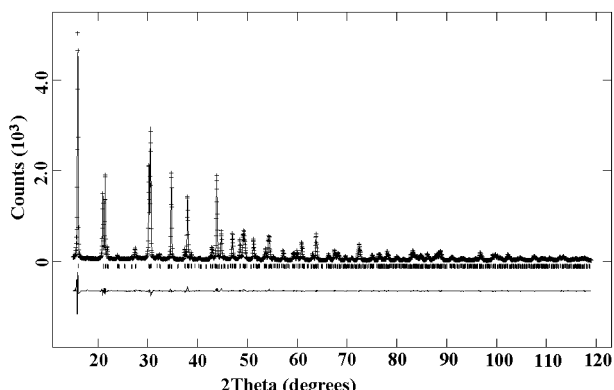


**Figure 1.** Profile fit to the powder X-ray diffraction pattern of  $\text{GdB}_5\text{O}_9$ . The symbol + represents the observed pattern, solid line represents the calculated pattern; the marks below the diffraction patterns are the calculated reflection positions and the difference curve is shown at the bottom of the figure.

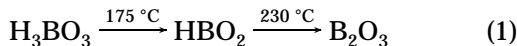
**Table 4. Atomic Coordinates and Thermal Displacement Parameters in  $\text{GdB}_5\text{O}_9$**

atom	site	<i>x</i>	<i>y</i>	<i>z</i>	<i>U</i> (eq)
Gd1	16d	0	0	0.193806(21)	0.00176(14)
O1	32g	-0.5289(11)	0.2036(17)	0.17275(24)	0.0030(8)
O2	16d	1/2	0	0.12439(19)	0.0030(8)
O3	32g	-0.3001(17)	0.0298(12)	0.17786(24)	0.0030(8)
O4	16f	-0.1229(6)	0.1229(6)	1/4	0.0030(8)
O5	16e	1/4	0.1648(11)	1/8	0.0030(8)
O6	32g	0.1645(8)	0.2392(7)	0.21743(18)	0.0030(8)
B1	16f	-0.2328(16)	0.2328(16)	1/4	0.0061(25)
B2	32g	-0.6287(21)	0.0912(20)	0.1462(4)	0.0061(25)
B3	32g	-0.3916(18)	0.1557(15)	0.1897(5)	0.0061(25)

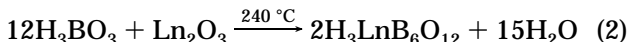
**Table 5. Selected Bond Distances (Å) and Angles (deg) in  $\text{GdB}_5\text{O}_9$**

bond distance (Å)		bond angles (deg)	
Gd1–O1	2	2.553(14)	O4–B1–O6 122.8(7)
Gd1–O2		2.294(6)	O6–B1–O6 114.3(14)
Gd1–O3	2	2.542(13)	O1–B2–O2 102.2(12)
Gd1–O4	2	2.372(4)	O1–B2–O3 100.9(9)
Gd1–O6	2	2.520(6)	O1–B2–O5 115.4(12)
B1–O4		1.280(19)	O2–B2–O3 106.2(10)
B1–O6	2	1.403(11)	O1–B3–O3 125.6(13)
B2–O1		1.527(17)	O1–B3–O6 113.4(12)
B2–O2		1.492(12)	O3–B3–O6 120.4(14)
B2–O3		1.573(17)	
B2–O5		1.369(13)	
B3–O1		1.327(17)	
B3–O3		1.342(17)	
B3–O6		1.354(14)	

acid to  $\text{B}_2\text{O}_3$  is shown as follows:



This condensation process is reversible in a closed system. In the presence of rare earth oxides, however, hydrated rare earth polyborates are formed with almost quantitative yield. For the rare earth oxides from Sm to Lu, the products are hydrated hexaborates and the reaction can be expressed as



A similar reaction is applicable for the early rare earth

(23) Strong, S. L.; Wells, A. F.; Kaplow, R. *Acta Crystallogr.* **1971**, *B27*, 1662.

(24) Prewitt, C. T.; Shannon, R. D. *Acta Crystallogr.* **1968**, *B24*, 869.

**Table 6. Unit Cell Parameters of  $\text{H}_3\text{LnB}_6\text{O}_{12}$  and  $\text{LnB}_5\text{O}_9$**

	$\text{H}_3\text{LnB}_6\text{O}_{12}$		$\text{LnB}_5\text{O}_9$	
	<i>a</i> (Å)	<i>c</i> (Å)	<i>a</i> (Å)	<i>c</i> (Å)
Sm	8.4336(2)	20.8003(4)	8.2789(4)	33.7320(16)
Eu	8.4191(1)	20.7745(2)	8.2556(2)	33.6625(13)
Gd <sup>a</sup>	8.4081(1)	20.7426(2)	8.2381(6)	33.6377(4)
Tb	8.3952(1)	20.7094(3)	8.2178(2)	33.5759(11)
Dy	8.3895(1)	20.6687(4)	8.2033(2)	33.5165(12)
Ho	8.3825(1)	20.6276(2)	8.1769(2)	33.4525(16)
Er	8.3698(1)	20.5848(6)	8.1546(8)	33.4176(63)
Tm	8.3605(2)	20.5404(7)		
Yb	8.3580(8)	20.5089(33)		
Lu	8.3506(10)	20.4756(46)		

<sup>a</sup> The lattice constants were obtained by powder data, which are not very different from those obtained from single-crystal diffraction.

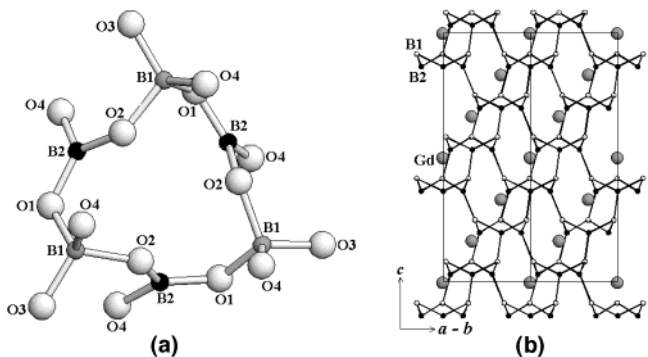


**Figure 2.** (a) Fundamental structure fragment of  $\text{B}_6\text{O}_{15}$  in  $\text{H}_3\text{GdB}_6\text{O}_{12}$ ; (b) polyborate framework in  $\text{H}_3\text{GdB}_6\text{O}_{12}$  showing only the rare earth cations and the connection of the borate groups.

oxides. In such cases, two new rare earth polyborates, that is, octaborates (La–Nd) and nonaborates (Nd–Sm), were obtained. The characterization of these compounds is underway and will be published elsewhere.

Most of the products are single phases, but a small amount of unknown impurity was present in the samples from Er to Lu. The cell parameters of  $\text{H}_3\text{LnB}_6\text{O}_{12}$  exhibit a gradual decrease from Sm to Lu as shown in Table 6 due to the lanthanide contraction. All of the hydrated rare earth hexaborates are isostructural to  $\text{H}_3\text{GdB}_6\text{O}_{12}$ , consisting of a six-membered ring of  $\text{B}_6\text{O}_{15}$  as the fundamental borate fragment. As shown in Figure 2a, this fragment contains an equal number of  $\text{BO}_3$  and  $\text{BO}_4$  groups that are linked alternatively, forming a six-membered ring. Nine terminal oxygen atoms are present in the  $\text{B}_6\text{O}_{15}$  unit; three of them are from  $\text{BO}_3$  and six from  $\text{BO}_4$ . All terminal oxygen atoms on  $\text{BO}_3$ , as well as half on  $\text{BO}_4$ , are further connected to the neighboring  $\text{B}_6\text{O}_{15}$  rings, so the 3D structure of  $\text{H}_3\text{GdB}_6\text{O}_{12}$  is featured in the three vertexes sharing  $\text{BO}_3$  and  $\text{BO}_4$ . The structure refinement was not able to locate the hydrogen atoms, but the bond-valence sums calculation<sup>25</sup> shows a significant deviation from -2 at the O3 position (BVS = -1.2). Furthermore, the valence summation at the Gd position is relatively high (BVS = +3.5), indicating that extra positive charge might be present in this region. In this sense, the borate framework can be expressed as  $3[\{\text{BO}_{3/2}\}^0|\text{BO}_{3/2}\text{OH}^-]$ , where the negative charge is localized mostly on the  $\text{BO}_4$

(25) Brese, N. E.; O'Keeffe, M. *Acta Crystallogr.* **1991**, *B 47*, 192.

(26) Saubat, B.; Vlasse, M.; Fouassier, C. *J. Solid State Chem.* **1980**, *34*, 271.

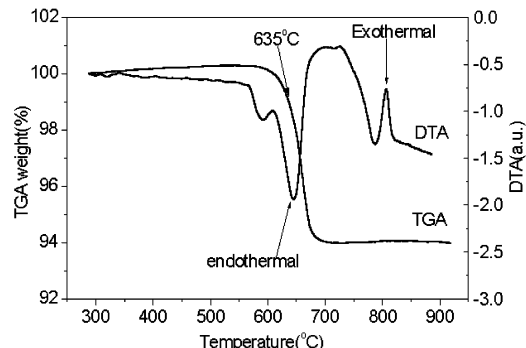


**Figure 3.** DTA and TGA curves of  $\text{H}_3\text{GdB}_6\text{O}_{12}$ .

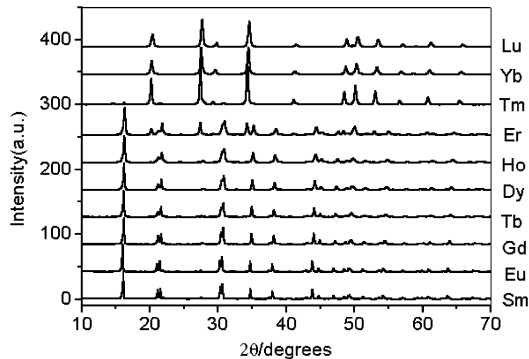


**Figure 4.** Powder X-ray diffraction patterns of the decomposition products of  $\text{H}_3\text{LnB}_6\text{O}_{12}$  with annealing at 650–700 °C. The anhydrous pentaborates  $\text{LnB}_5\text{O}_9$  were formed for  $\text{Ln} = \text{Sm}–\text{Ho}$ , and the orthoborates  $\text{LnBO}_3$  were observed for  $\text{Ln} = \text{Yb}–\text{Lu}$ . The decomposition products of  $\text{H}_3\text{ErB}_6\text{O}_{12}$  and  $\text{H}_3\text{TmB}_6\text{O}_{12}$  are mixtures containing both  $\text{LnB}_5\text{O}_9$  and  $\text{LnBO}_3$ .

groups. To compensate for the negative charge, the hydroxyl groups are further coordinated to the gadolinium atom with a bond distance of 2.392 Å (Gd–O3). Comparatively, in anhydrous polyborates, the negative charges are more delocalized. For example, the borate anion  $[\text{B}_5\text{O}_{10}]^{5-}$  in  $\text{LaMgB}_5\text{O}_{10}$ <sup>26</sup> exhibits a layered structure in which  $\text{BO}_4$  is four-vertexes connected and  $\text{BO}_3$  is only two-vertexes connected, and therefore, the negative charges are equally distributed in all borate groups as  $\{[\text{BO}_{4/2}]^-\}_3\{[\text{BO}_{2/2}\text{O}]^-\}_2$ .

Figure 2b shows an overview of the framework in  $\text{H}_3\text{GdB}_6\text{O}_{12}$ . To emphasize the overall connection in the structure, only the boron and gadolinium atoms are illustrated. The overall structure of  $\text{H}_3\text{GdB}_6\text{O}_{12}$  could be understood in such a way that the  $\text{B}_6\text{O}_{15}$  units, by thinking them as pseudoatoms, form a close-packed layer (not bonded), which are further stacked as the cubic close-packed array along the  $c$  axis. The  $\text{B}_6\text{O}_{15}$  units are bonded directly to the six neighbors in the adjacent layers forming a 3D framework. Such a structure arrangement yields additional six- and ten-membered rings as shown in Figure 2b. The polyborate anion  $[\text{B}_6\text{O}_{15}]^{6-}$  itself is an open framework; however, the cavities in the framework are filled by the rare earth atoms that are coordinated by nine oxygen atoms with a tricapped trigonal prismatic polyhedron.

$\text{H}_3\text{GdB}_6\text{O}_{12}$  decomposes at about 635 °C, accompanied by a significant weight loss as shown in Figure 3. At the initial stage of the decomposition, an amorphous phase was formed, which was then crystallized by additional heat treatment. Figure 4 shows the powder X-ray diffraction patterns of the  $\text{H}_3\text{LnB}_6\text{O}_{12}$  samples

after annealing at 650–700 °C for 5 days. Depending on the ionic radii of the rare earth, two different crystalline products were obtained.  $\text{LnB}_5\text{O}_9$  is formed for larger rare earths from Sm to Ho. Meanwhile, for the smaller rare earths ( $\text{Ln} = \text{Yb}–\text{Lu}$ ),  $\text{H}_3\text{LnB}_6\text{O}_{12}$  decomposes directly to orthoborate  $\text{LnBO}_3$ . The decomposition products of  $\text{H}_3\text{ErB}_6\text{O}_{12}$  and  $\text{H}_3\text{TmB}_6\text{O}_{12}$  are mixtures containing both  $\text{LnB}_5\text{O}_9$  and  $\text{LnBO}_3$ .  $\text{LnB}_5\text{O}_9$  is dominant for  $\text{Ln} = \text{Er}$  whereas  $\text{LnBO}_3$  is dominant for  $\text{Ln} = \text{Tm}$ , even if the annealing treatment proceeded as low as 650 °C. The corresponding reactions can be expressed as



The weight loss expected from the above equations is 6.473 wt % for  $\text{H}_3\text{GdB}_6\text{O}_{12}$ , which agrees reasonably well with the observed value in the TGA study (6.04 wt %).  $\text{B}_2\text{O}_3$  in the product may exist in noncrystalline form, so it does not appear in the diffraction patterns.

All other pentaborates  $\text{LnB}_5\text{O}_9$  are isostructural to  $\text{GdB}_5\text{O}_9$  crystallized in a tetragonal structure. The lattice constants decrease continuously from  $\text{SmB}_5\text{O}_9$  to  $\text{ErB}_5\text{O}_9$  due to the lanthanide contraction (Table 6). The borate framework in  $\text{LnB}_5\text{O}_9$  consists of  $\text{B}_4\text{O}_9$  and  $\text{BO}_3$  as the fundamental fragments. The  $\text{B}_4\text{O}_9$  is a double three-membered ring unit formed by two  $\text{BO}_3$  and two  $\text{BO}_4$ . The  $\text{B}_4\text{O}_9$  unit is known as a common fundamental fragment in metal polyborates. For example, the Borax ( $\text{Na}_2[\text{B}_4\text{O}_5(\text{OH})_4] \cdot 8\text{H}_2\text{O}$ ) contains an isolated  $\text{B}_4\text{O}_5(\text{OH})_4$  unit<sup>17</sup> in which terminal O atoms bond to hydrogen as the hydroxyl groups. In the structure of  $\text{GdB}_5\text{O}_9$ , the  $\text{B}_4\text{O}_9$  units are linked via terminal oxygen (on  $\text{BO}_4$ ), forming a one-dimensional chain (Figure 5a). The other two terminal O atoms (on  $\text{BO}_3$ ) are further connected to the additional  $\text{BO}_3$  group forming the three-dimensional framework. The 3D framework of  $\text{B}_5\text{O}_9^{3-}$  can, therefore, be expressed as  $\{[\text{BO}_{3/2}]_2[\text{BO}_{4/2}]_2[\text{BO}_{2/2}\text{O}]_2\}^{3-}$ . Figure 5b shows a projection of the structure of  $\text{GdB}_5\text{O}_9$ . It can be seen that the  $\text{BO}_3$  and  $\text{BO}_4$  groups are connected to form a 3D framework and the Gd atoms occupy the cavities in the framework. The coordination polyhedron of gadolinium is a distorted three-capped trigonal prism.

According to the Lux-Flood acid–base concept, the 3D framework in  $\text{LnB}_5\text{O}_9$  may not be very stable because of the high valence of rare earth (III); it may decompose to isolated or low-dimensional borate units at high temperature. It was found that the  $\text{LnB}_5\text{O}_9$  decomposes at high temperature to metaborates or orthoborates. Figure 6 shows a phase diagram for the rare earth borate system. The two critical temperatures, that is,  $T_{d1}$  and  $T_{d2}$ , are respectively the temperature of weight loss, characteristic for the dehydration of  $\text{H}_3\text{LnB}_6\text{O}_{12}$ , and the decomposition temperature of  $\text{LnB}_5\text{O}_9$  to orthoborates or metaborates.  $T_{d1}$  is almost constant for all rare earth systems, indicating that the thermal stability is similar for the hydrated hexaborates  $\text{H}_3\text{LnB}_6\text{O}_{12}$ .  $T_{d2}$ , on the other hand, depends on the rare earth cations; it increases slightly from Sm to Tb and then decreases as the ionic radii become smaller. It should be noted that the highest decomposition temperature  $T_{d2}$  appeared at the Tb, which coincides with the smallest rare

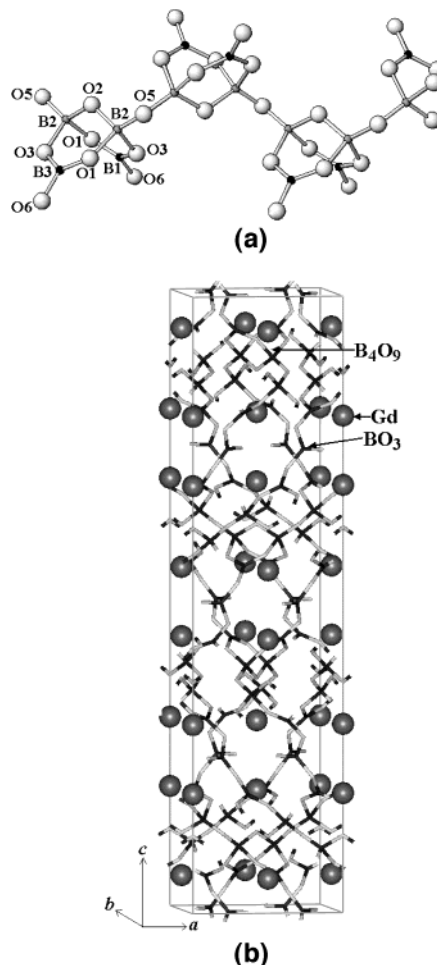


**Figure 5.** (a) The fundamental borate fragment  $B_4O_9$  in anhydrous pentaborate  $LnB_5O_9$ , which forms a one-dimensional chain by sharing the oxygen atoms on the  $BO_4$  group; (b) crystal structure of  $LnB_5O_9$ , where the rare earth cations are expressed as balls and the borate network is displayed in line style.

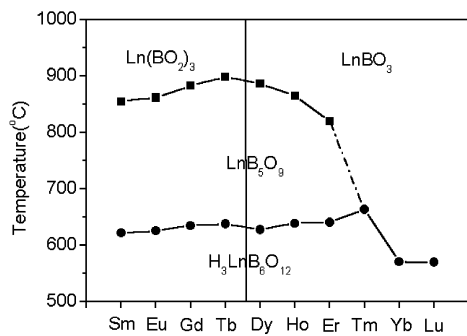


**Figure 6.** Phase diagram of the rare earth polyborates.  $T_{d1}$  represents the dehydration temperature of  $H_3LnB_6O_{12}$  and  $T_{d2}$  represents the decomposition temperature from  $LnB_5O_9$  to  $Ln(BO_2)_3$  or  $LnBO_3$  that are separated by a vertical line.

earth for the metaborates. The observed decomposition products of  $LnB_5O_9$  are indeed the metaborates from Sm to Tb and the orthoborates from Dy to Er. The lower dehydration temperature for the two smallest rare earths (Yb and Lu) is presumably related to that the decomposition of  $H_3LnB_6O_{12}$  that yields directly to orthoborates. Tm is on the borderline so that only a trace of  $TmB_5O_9$  was observed, even if the decomposition reaction proceeded at 650 °C. The  $LnB_5O_9$  is a well-

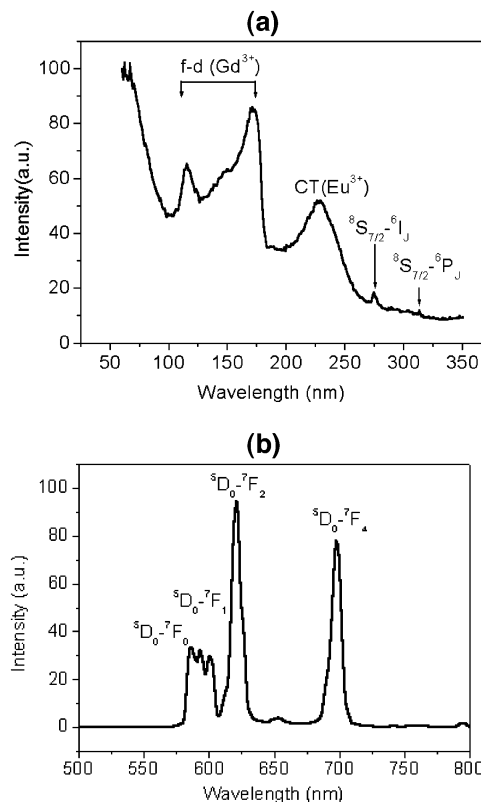


**Figure 7.** (a) Excitation spectrum ( $\lambda_{em} = 615$  nm) and (b) emission spectrum ( $\lambda_{ex} = 125$  nm) of  $GdB_5O_9:Eu$ .

defined compound in the  $Ln_2O_3-B_2O_3$  system. The absence of this phase in the  $Ln_2O_3-B_2O_3$  phase diagram<sup>2</sup> is largely due to the low decomposition temperatures. Furthermore, the borate-rich system has a strong tendency to form a glassy phase at high temperature; thus, the syntheses of polyborates are practically difficult by using the conventional high-temperature techniques.

Europium-doped material  $GdB_5O_9:Eu^{3+}$  was prepared by using the same method as described for the pure compound, except a certain amount of  $Eu_2O_3$  was added in the reaction systems. Figure 7 shows the excitation and emission spectra of  $GdB_5O_9:Eu^{3+}$ . The excitation spectrum was measured in a vacuum ultraviolet (VUV) range by monitoring the  $Eu^{3+}$  emission at 615 nm. The excitation transitions in the spectrum can be categorized into two parts. The strong excitation band at about 120–150 nm and the sharp peaks at 275 and 315 nm originate from the f–d,  $^8S_{7/2}-^6I_J$ , and  $^8S_{7/2}-^6P_J$  transitions of  $Gd^{3+}$ , respectively. Another broad excitation band at about 230–260 nm originates from the charge-transfer transition (CT) of  $O \rightarrow Eu^{3+}$ . The appearance of  $Gd^{3+}$  absorption in the excitation spectrum implies an effective energy transfer between  $Gd^{3+}$  and  $Eu^{3+}$  in this material, which is very important for the luminescent materials used under the excitation of high-energy photons. The emission spectrum (Figure 7b) consists of mainly the  $^5D_0-^7F_0$ ,  $^5D_0-^7F_1$ ,  $^5D_0-^7F_2$ , and  $^5D_0-^7F_4$  transitions. Because the Gd atoms in  $GdB_5O_9$  occupy an ancentrosymmetric site (local symmetry is  $C_2$ ), the electric dipole–dipole transition of  $^5D_0-^7F_2$  is predominant in this material. The concentration quenching of the  $Eu^{3+}$  emission is significantly high for this material. As shown in Figure 8, the emission intensity of  $GdB_5O_9:$

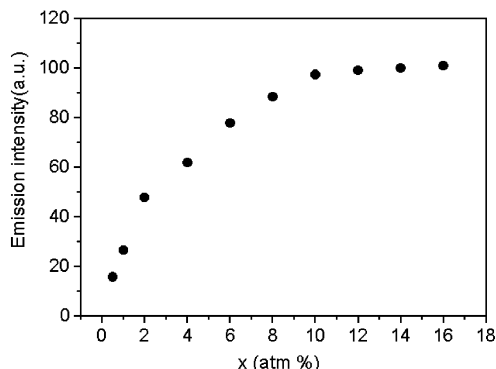


**Figure 8.** Variation of the emission intensity on the doping concentration in the  $\text{GdB}_5\text{O}_9:\text{Eu}$  system. The  $x$  value represents the doping concentration in  $\text{Gd}_{1-x}\text{Eu}_x\text{B}_5\text{O}_9$ .

$\text{Eu}^{3+}$  increases with the doping concentration up to  $x = 0.1$  and then remains almost constant beyond this doping level.

In summary, molten boric acid is an effective reaction medium for syntheses of the hydrated rare earth hexaborates  $\text{H}_3\text{LnB}_6\text{O}_{12}$  ( $\text{Ln} = \text{Sm-Lu}$ ). Careful annealing of the hexaborates at 650–700 °C results in the

formation of anhydrous pentaborates  $\text{LnB}_5\text{O}_9$  ( $\text{Ln} = \text{Sm-Er}$ ). The pentaborates are metastable, so they cannot be synthesized by conventional high-temperature reaction. The preparation strategy for the anhydrous rare earth polyborates proposed here is in fact a precursor method in which the hydrated polyborates are the precursors first prepared in molten boric acid. Then the anhydrous rare earth polyborates are obtained by annealing the precursors at mild conditions. It is believed that this approach will be useful for exploring polyborate chemistry of rare earth and other high valence cations.

**Acknowledgment.** We are thankful for the financial support from NSFC and the State Key Basic Research Program of China.

**Supporting Information Available:** Crystallographic information files for  $\text{H}_3\text{GdB}_6\text{O}_{12}$  and  $\text{GdB}_5\text{O}_9$  (CIF). This material is available free of charge via the Internet at <http://pubs.acs.org>.

CM0203870